VIRTUAL SENSORS FOR ROBUST ON-LINE MONITORING (OLM) AND DIAGNOSTICS

Ramakrishna Tipireddy, Megan Lerchen, and Pradeep Ramuhalli*
Pacific Northwest National Laboratory
P.O. Box 999, Richland, WA, 99352 USA
Ramakrishna.Tipireddy@pnnl.gov; Megan.Lerchen@pnnl.gov; Pradeep.Ramuhalli@pnnl.gov

ABSTRACT

Unscheduled shutdown of nuclear power facilities for recalibration and replacement of faulty sensors can be expensive and disruptive to grid management. In this work, we present virtual (software) sensors that can replace a faulty physical sensor for a short duration thus allowing recalibration to be safely deferred to a later time. The virtual sensor model uses a Gaussian process model to process input data from redundant and other nearby sensors. Predicted data includes uncertainty bounds including spatial association uncertainty and measurement noise and error. Using data from an instrumented cooling water flow loop testbed, the virtual sensor model has predicted correct sensor measurements and the associated error corresponding to a faulty sensor.

Key Words: Online monitoring (OLM), Virtual sensors, Gaussian process model

1 INTRODUCTION

Process sensors in nuclear power facilities are regularly calibrated to ensure reliable measurements as part of routine, scheduled maintenance. When checked, however, these sensors are frequently found to be within calibration and that recalibration was unnecessary [1]. When a faulty sensor is found in an operating plant, the facility shuts down ahead of the next scheduled maintenance outage.

Online monitoring (OLM) of sensors is one approach that the nuclear industry is evaluating for diagnosis of sensor faults based on operating plant data [2, 3, 4]. Condition-based sensor maintenance schedules could extend or eliminate the need for scheduled sensor calibration by continuously assessing the health of plant sensors while the facility is operating. Further, available sensor data from a virtual or software sensor reading could replace the measurement from the faulty sensor for a short duration, thereby extending the up-time of the plant while safely deferring the faulty sensor's calibration.

Key issues for development of a virtual sensor measurement capability (predicted measurement) include the accuracy of the predicted measurement, the uncertainty associated with the predicted measurement, and the ability to confidently assure this predicted reading remains within the plant set-points and acceptance criteria. In this paper, we focus on defining a methodology where the virtual sensor data can be accurately predicted within defined uncertainty bounds.

*Corresponding author

2 VIRTUAL SENSORS

A virtual sensor is a software tool that uses measured data from available physical sensors and predicts the process output associated with a particular sensor. The virtual sensor-predicted data can be used in monitoring sensor performance and to replace the output from a faulty sensor. Virtual sensors are used or are being developed for use in many applications, including: glucose monitoring in non-insulin-dependent people [5], active noise control for virtual microphones [6], nuclear power plants [1, 7, 8], mechanical systems [9], thermal management of a microprocessor chip [10], and many others.

Various approaches have been used for virtual sensor development. Data mining-based virtual sensors are presented in [11]. In [12] Kalman filtering is used as a virtual sensor that can predict the properties of a structural system by measuring multiple sources of data. In [13] a fuzzy support vector regression is used for a soft sensing model of a feed water flow rate in a pressurized water reactor.

In this work, we used a Bayesian method to estimate parameters for constructing Gaussian process models [14] for virtual sensor development. We elected to use this approach for its ability to predict the sensor output, including associated spatial uncertainty and measurement noise. In particular, we follow the multi-output separable Gaussian process developed in [15, 16].

To validate our Gaussian process model, we first use the measurements from healthy sensors as training data to estimate the model parameters and then use these parameters in the Gaussian process regression to predict the process data and uncertainty bounds corresponding to the faulty sensor. We assume that the faulty sensor is detected using other fault detection techniques.

3 GAUSSIAN PROCESS (GP) MODELS

In this section, we describe a multi-output Gaussian process [17] model used as a virtual sensor for predicting the measurement of a faulty sensor. Here, the Gaussian process model is constructed for data corresponding to the faulty sensor as a function of the measurement data from redundant and/or nearby healthy sensors. First, the GP model is constructed from the training data, when all the sensors are functioning properly. When a sensor fails, we use the GP model to predict its correct process measurement from the test data from other physical sensors. In the rest of the section, we describe the mathematical equations for GP models, methods to estimate the parameters of the GP models, and prediction of unknown quantities (here data corresponding to faulty sensors) from using GP models.

Let $\boldsymbol{x} \in \mathcal{X} \subset \mathbb{R}^p$ and $\boldsymbol{y} \in \mathbb{R}^q$ be multi-variate input and output variables, respectively. In this approach, we use training data $D = \{(\boldsymbol{x}_i, \boldsymbol{y}_i = f(\boldsymbol{x}_i)), i = 1, \cdots, n\}$ consisting of n observations to construct the Gaussian process model and use Gaussian process regression to predict the output values $\boldsymbol{y}^*$ corresponding to the input values $\boldsymbol{x}^*$. Here $f : \mathcal{X} \mapsto \mathbb{R}^q$ can be any real valued function, a simulator, or an experiment that takes input $\boldsymbol{x}$ and gives output $\boldsymbol{y} = f(\boldsymbol{x})$. Let $\boldsymbol{X} = \{\boldsymbol{x}_1, \cdots, \boldsymbol{x}_n\}$ and $\boldsymbol{Y} = \{\boldsymbol{y}_1, \cdots, \boldsymbol{y}_n\}$ be the input and output observations respectively, from the training data D. In the GP model, conditional distribution $p(\boldsymbol{Y}|\boldsymbol{X})$ describes the dependence of observable $\boldsymbol{Y}$ on corresponding input $\boldsymbol{X}$. In a Bayesian setting, following the notation in [17], we represent the unknown function $f(\cdot)$ with a q-dimensional Gaussian process,

$$f(\cdot)|B, \Sigma, \theta \sim \mathcal{N}_q(m(\cdot), c(\cdot, \cdot)\Sigma) \tag{1}$$

conditioned on hyper parameters, $B \in \mathbb{R}^{n \times q}$ and $\Sigma \in \mathbb{R}^{q \times q}$ and θ representing the parameters of the correlation function $c(\cdot, \cdot, \theta)$. Eq. 1 says that $f(\cdot)|B, \Sigma, \theta$ follows Gaussian distribution with mean and correlation function as follows,

$$\mathrm{E}[f(\boldsymbol{x})|B,\Sigma,\theta] = m(\boldsymbol{x},B), \tag{2}$$

and

$$\mathrm{Cov}[f(\boldsymbol{x}_1), f(\boldsymbol{x}_2)|B,\Sigma,\theta] = c(\boldsymbol{x}_1,\boldsymbol{x}_2,\theta)\Sigma. \tag{3}$$

Here, we use generalized linear model for mean [16] as,

$$m(\boldsymbol{x};B) = B^T\boldsymbol{h}(\boldsymbol{x}), \tag{4}$$

where, $\boldsymbol{h} : \mathcal{X} \mapsto \mathbb{R}^r$, $\boldsymbol{h}(\boldsymbol{x}) = \{h_1(\boldsymbol{x}),\cdots,h_r(\boldsymbol{x})\}$ are regression functions corresponding to each component of $f(\boldsymbol{x})$ and $B = \{\beta_1,\cdots,\beta_q\}$ is a matrix of regression coefficients. We assume that the parameters (B,Σ) and θ are independent such that,

$$\pi(B,\Sigma,\theta) = \pi(B,\Sigma)\pi(\theta), \tag{5}$$

where $\pi(\theta)$ is the prior distribution of θ and $\pi(B,\Sigma)$ is a joint prior that we assume as non-informative prior [17],

$$\pi(B,\Sigma) \propto |\Sigma|^{-\frac{q+1}{2}}. \tag{6}$$

We choose following exponential correlation function,

$$c(\boldsymbol{x}_1,\boldsymbol{x}_2) = \exp\left\{-\frac{1}{2}\sum_{j=1}^{q}\frac{(x_k^{(1)}-x_k^{(2)})^2}{\lambda^2}\right\} + g^2\delta_{\boldsymbol{x}_1,\boldsymbol{x}_2}, \tag{7}$$

where, λ is the correlation length and g is nugget quantity used for stability of the correlation matrix.

Given the input $\boldsymbol{X} \in \mathbb{R}^{n\times p}$ and output $\boldsymbol{Y} \in \mathbb{R}^{n\times p}$ data, the likelihood is given by

$$(\boldsymbol{Y}|B,\Sigma,\theta) \sim \mathcal{N}_{n\times q}(HB,\Sigma,A), \tag{8}$$

where,

$$H = \{\boldsymbol{h}(\boldsymbol{x}_1,\cdots,\boldsymbol{h}(\boldsymbol{x}_n\}^T \in \mathbb{R}^{n\times r} \tag{9}$$

is the design matrix and

$$A = (c(\boldsymbol{x}_i,\boldsymbol{x}_j;\theta)) \in \mathbb{R}^{n\times n} \tag{10}$$

is the covariance matrix. Then the predictive distribution $f(\cdot|B,\Sigma,\theta,\boldsymbol{Y})$ is,

$$f(\cdot|B,\Sigma,\theta,\boldsymbol{Y}) = \mathcal{N}_q(m^*(\cdot,B), c^*(\cdot,\cdot;\theta)\Sigma), \tag{11}$$

where,

$$m^*(\boldsymbol{x};B) = B^T\boldsymbol{h}(\boldsymbol{x}) + (\boldsymbol{Y}-HB)^T A^{-1}a(\boldsymbol{x}) \tag{12}$$

and

$$c^*(\boldsymbol{x}_1,\boldsymbol{x}_2;\theta) = c(\boldsymbol{x}_1,\boldsymbol{x}_2;\theta) - a^T(\boldsymbol{x}_1)A^{-1}a(\boldsymbol{x}_2), \tag{13}$$

where, $a(\boldsymbol{x}) = \{c(\cdot,\boldsymbol{x}_1;\theta),\cdots,c(\cdot,\boldsymbol{x}_n;\theta)\} \in \mathbb{R}^n$. If $n > r+q$; that is, if all the distributions involved are proper, it is possible to integrate out B and Σ resulting in predictive distribution $f(\cdot)$ that is conditional only on θ, which is a q-variate Student process with $n-r$ degrees of freedom [16, 17], that is

$$f(\cdot|\theta,\boldsymbol{Y}) = \mathcal{T}_q(m^{**}(\cdot,B), c^{**}(\cdot,\cdot;\theta)\hat{\Sigma}; n-r), \tag{14}$$

where,

$$m^{**}(\boldsymbol{x}) = \hat{B}^T \boldsymbol{h}(\boldsymbol{x}) + (\boldsymbol{Y} - H\hat{B})^T A^{-1} a(\boldsymbol{x}) \tag{15}$$

and

$$c^{**}(\boldsymbol{x}_1, \boldsymbol{x}_2; \theta) = c^*(\boldsymbol{x}_1, \boldsymbol{x}_2; \theta) - \hat{a}^T(\boldsymbol{x}_1)\hat{A}^{-1}\hat{a}(\boldsymbol{x}_2), \tag{16}$$

where,

$$\begin{aligned}
\hat{B} &= (H^T A^{-1} H)^{-1} H^T A^{-1} \boldsymbol{Y}, \\
\hat{a}(\boldsymbol{x}) &= \boldsymbol{h}(\boldsymbol{x}) - H^T A^{-1} a(\boldsymbol{x}) \\
\hat{A} &= (H^T A^{-1} H), \\
\hat{\Sigma} &= \frac{1}{n-r} (\boldsymbol{Y} - H\hat{B})^T A^{-1} (\boldsymbol{Y} - H\hat{B}).
\end{aligned} \tag{17}$$

The posterior distribution of the parameters θ after integrating out B and Σ from the joint posterior of B, Σ, and θ conditioned on $\boldsymbol{Y}$ is,

$$p(\theta|\boldsymbol{Y}) \propto \pi(\theta)|A|^{-\frac{q}{2}}|H^T A^{-1} H|^{-\frac{q}{2}}|\hat{\Sigma}|^{-\frac{n-r}{2}}. \tag{18}$$

The posterior $p(\theta|\boldsymbol{Y})$ can be sampled using Markov Chain Monte Carlo (MCMC) methods such as Gibb's sampling [18] or Metropolis Hasting's algorithm [19, 20].

4 EXPERIMENTAL DATA

We demonstrate virtual sensor models for experimental data acquired with an instrumented flow loop shown in Fig. 1 with varying test conditions. The flow loop consists of 17 sensors in which pressure and differential transmitters measure pressures and flows, respectively, and a combination of thermocouples and RTDs (resistance temperature detectors) measure temperatures. Training data is collected at 20 Hz frequency under 9 different temperature ($91, 96, 99, 100, 100, 105, 105, 108$, and 110^{o} F) conditions. Test data corresponding to process sensor FT-3-2 is drifted by turning the zero adjustment screw $1/4$ turn every 5 minutes as shown in Fig. 2. We demonstrate the virtual sensor methodology by predicting the correct test data for faulty sensor FT-3-2, using input from test data from other sensors such as control temperature, control pressure, FT-3-1, and a combination of these sensors. In the next section we show the predicted measurement data and prediction error for sensor FT-3-2 using Gaussian process models.

5 RESULTS AND DISCUSSION

Here, we show results indicating the potential for using the Gaussian process model as a virtual sensor. Fig. 2 shows the measurement of a faulty differential pressure sensor in which sensor drift (fault) is simulated by adjusting the calibration setting on the sensor every 5 minutes. Fig. 3 shows training data of process sensors FT-3-1 and FT-3-2 as a function of control temperature and control pressure. We can observe that the process sensors are very little sensitive to control pressure and it is not a good input data to predict FT-3-2 sensor data. We test the GP model prediction of FT-3-2 with various combinations of input data. Fig. 4a shows the predicted sensor data for FT-3-2 in black and lower and upper bounds in blue, where control pressure and control temperature are used as input data. In Fig. 4b, control pressure, control temperature, and FT-3-1 data are used as input to predict FT-3-2 measurement. We can observe that using only control

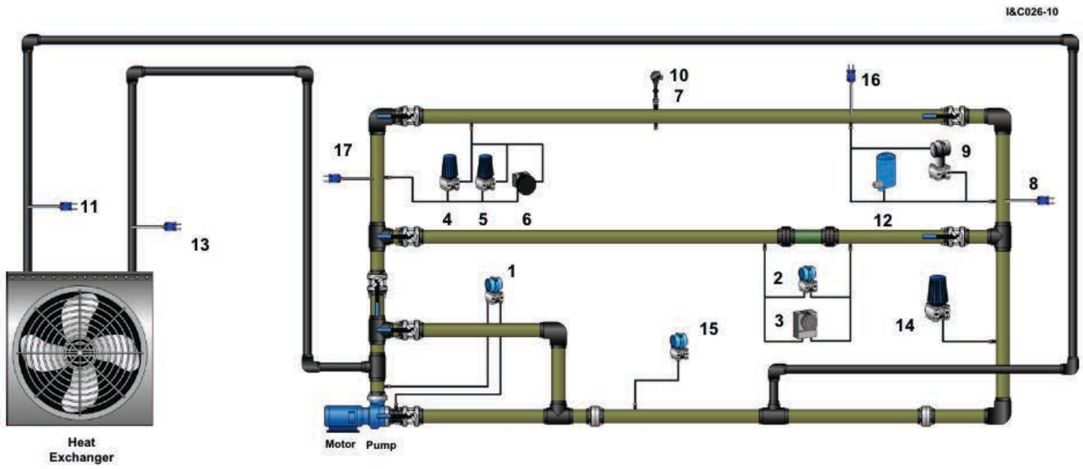

ITEM	ID	SENSOR TYPE	MANUFACTURER
1	FT-4-1	DIFFERENTIAL PRESSURE	ROSEMOUNT
2	FT-3-1	DIFFERENTIAL PRESSURE (SMART)	ROSEMOUNT
3	FT-3-2	DIFFERENTIAL PRESSURE	BARTON
4	FT-1-1	DIFFERENTIAL PRESSURE	FOXBORO
5	FT-1-2	DIFFERENTIAL PRESSURE	FOXBORO
6	FT-1-4	DIFFERENTIAL PRESSURE (SMART)	BARTON
7	TE-1-2	RTD (SMART)	ROSEMOUNT
8	TC-2-1	THERMOCOUPLE TYPE-J (SMART)	ROSEMOUNT
9	FT-2-1	DIFFERENTIAL PRESSURE	SCHLUMBERGER

ITEM	ID	SENSOR TYPE	MANUFACTURER
10	CTRL-TEMP	RTD (SMART)	ROSEMOUNT
11	TC-HX-OUT	THERMOCOUPLE TYPE-J	OMEGA
12	FT-2-3	DIFFERENTIAL PRESSURE	HONEYWELL
13	TC-HX-IN	THERMOCOUPLE TYPE-J	OMEGA
14	CTRL-PSR	GAUGE PRESSURE	FOXBORO
15	PT-2	GAUGE PRESSURE	ROSEMOUNT
16	TC-LOOP-FAR	THERMOCOUPLE TYPE-E	OMEGA
17	TC-PUMP-OUT	THERMOCOUPLE TYPE-K	OMEGA

Figure 1. Flow loop piping and instrumentation diagram

temperature and control pressure data is not good enough for accurate prediction, but the addition of FT-3-1 data gives a better prediction of FT-3-2. In Fig. 5a data from sensor FT-3-1 alone is used as input and in Fig. 5b data from FT-1-1 sensor alone is used as input. It shows that some sensors such as FT-3-1 are correlated well with the faulty sensor from which we can predict better results compared to less correlated input such as data from FT-1-1.

These results indicate that the predicted sensor reading has the potential for replacing the measurements from the faulty sensor. However, as seen in the graphic, approaches are needed for identifying the time at which the sensor begins drifting out of calibration. The impact of the prediction on plant operation (through potential adjustments to set-points) also needs further study.

6 CONCLUSIONS

Sensor calibration interval extension and signal validation in operating and new reactors can be achieved with improved, next-generation online monitoring (OLM) technologies. In this work we presented virtual sensors based on Gaussian process models that can replace faulty sensors for a period of time and thus postpone complete shutdown of the nuclear power facility. Faulty sensor data is simulated by turning the zero adjustment screw and is performed under steady state conditions. This results in faulty sensor data, but the process remains unchanged. Gaussian process models could accurately predict the process data using data from other sensor measurements. Gaussian process models are capable of predicting the process data even if it is changing due to different test conditions such as control pressure and control temperature. In the future, we will work with the data where the process is operated under 2 to 3 different test conditions.

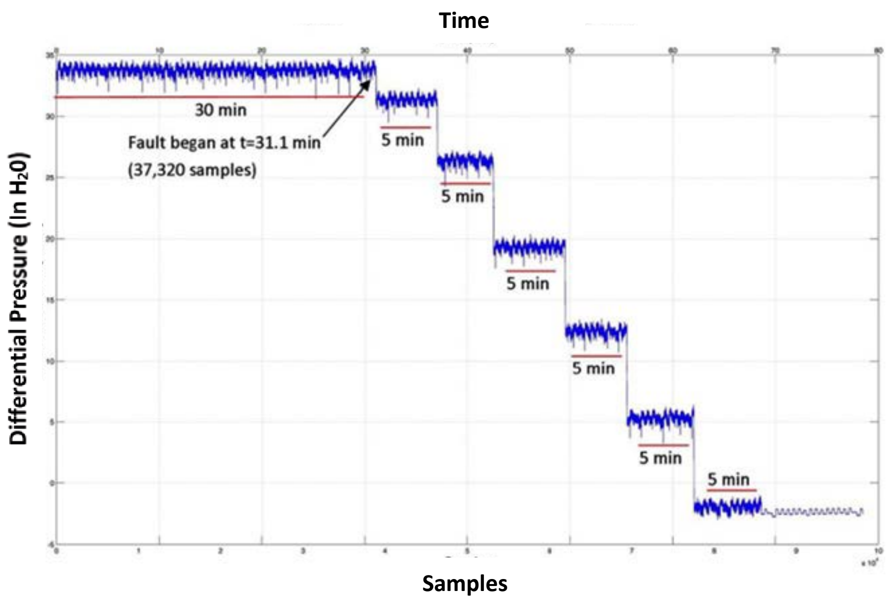

Figure 2. Process sensor FT-3-2 is drifted by turning the zero adjustment screw $1/4$ turn every 5 minutes.

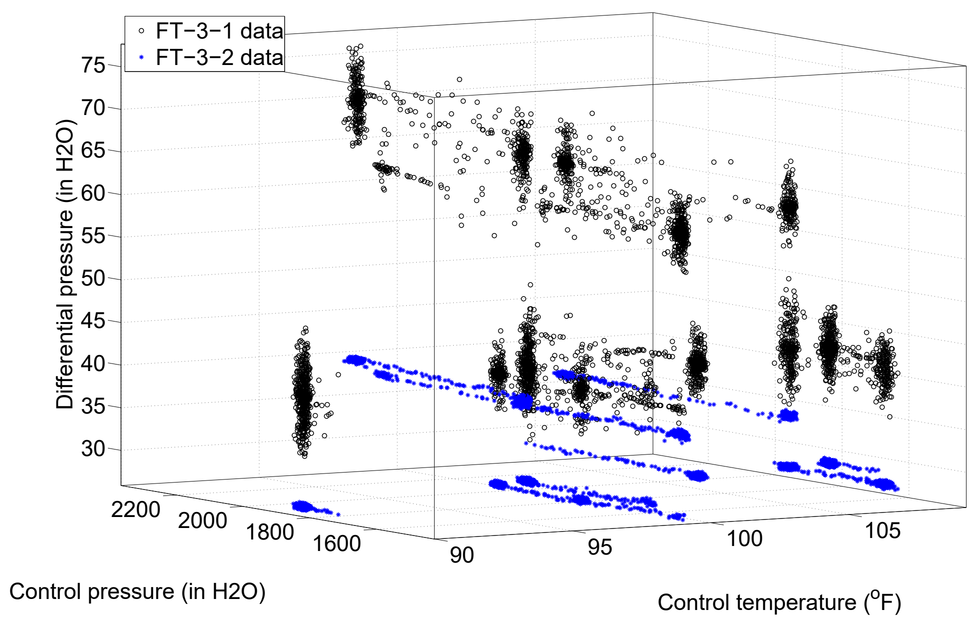

Figure 3. Training data of process sensors FT-3-1 and FT-3-2 as a function of control temperature and control pressure.

7 ACKNOWLEDGMENTS

The work described in this report was sponsored by the Advanced Sensors and Instrumentation (ASI) technical area within the Nuclear Energy Enabling Technologies (NEET) R&D program of the U.S. Department of Energy Office of Nuclear Energy. The authors thank Dr. Jamie Coble from the University of

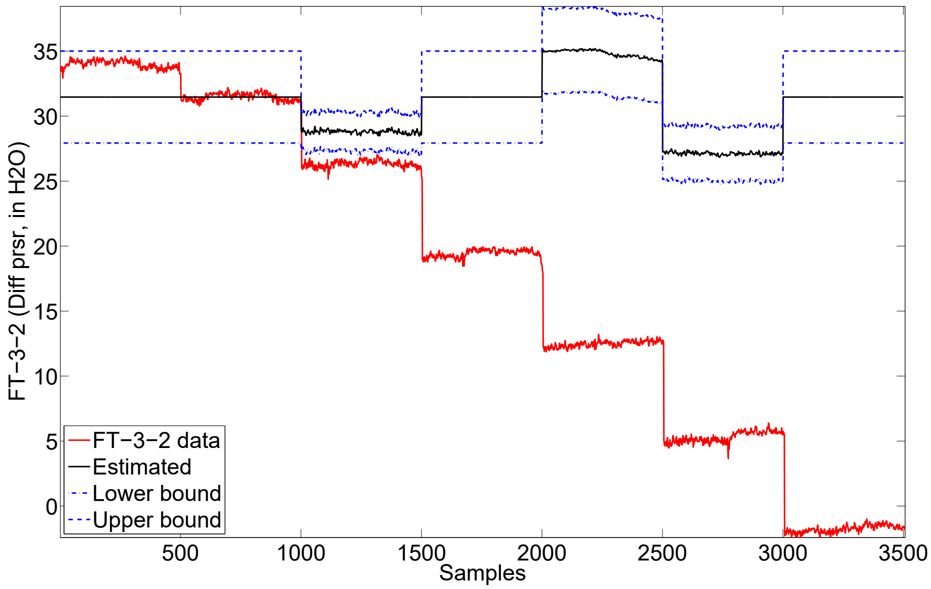

(a) input: temp and press

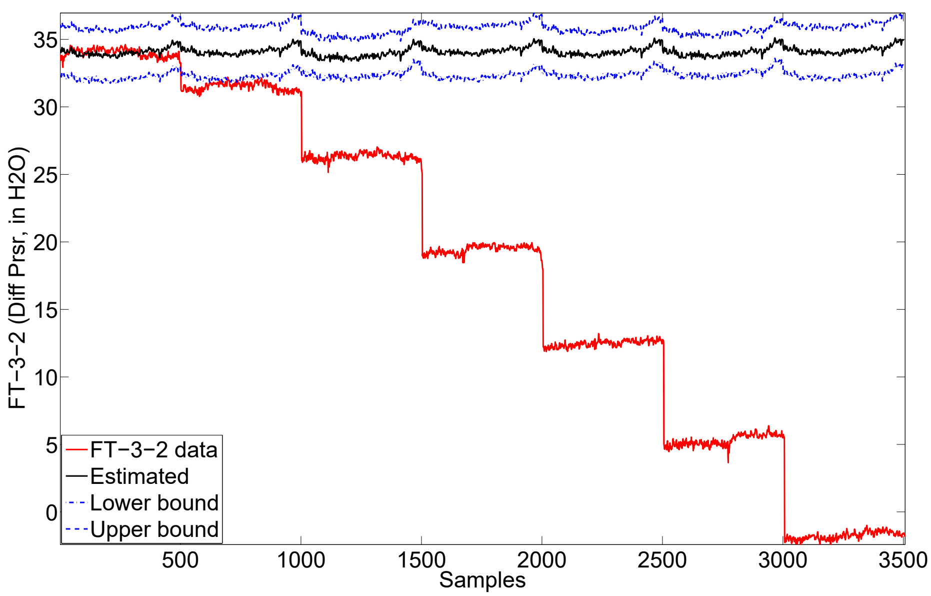

(b) input: temp, press and FT-3-1

Figure 4. GP model prediction for sensor FT-3-2 measurement using a) control temperature and control pressure as input and b) control temperature and control pressure and FT-3-1 as input.

Tennessee Knoxville, and Dr. Brent Shumaker and Dr. Hash Hashemian from AMS Corp., Knoxville, TN for their feedback on the research described here. The work described in this paper was performed at the Pacific Northwest National Laboratory, managed by Battelle for the U.S. Department of Energy under DOE contract number DE-AC06-76RLO-1830.

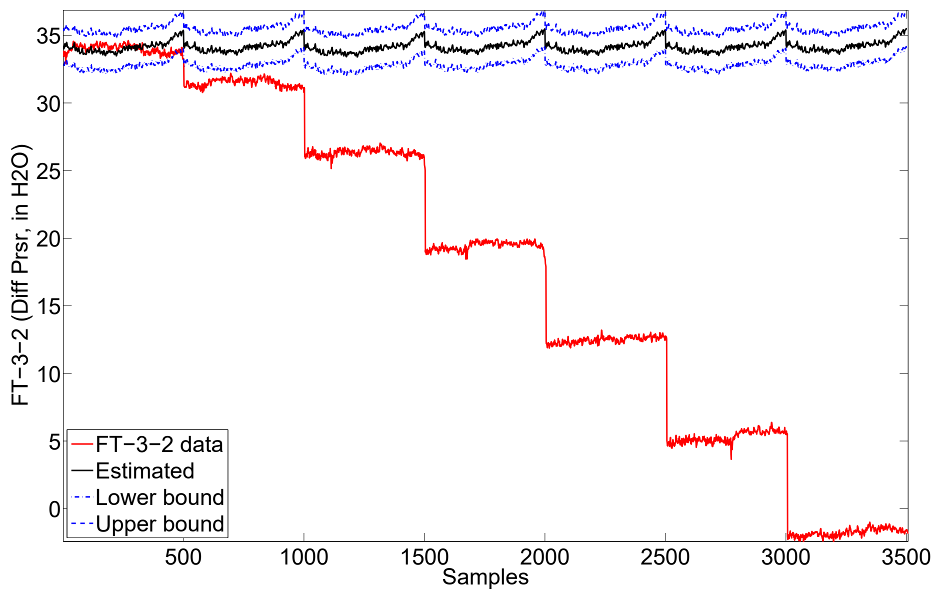

(a) input: FT-3-1

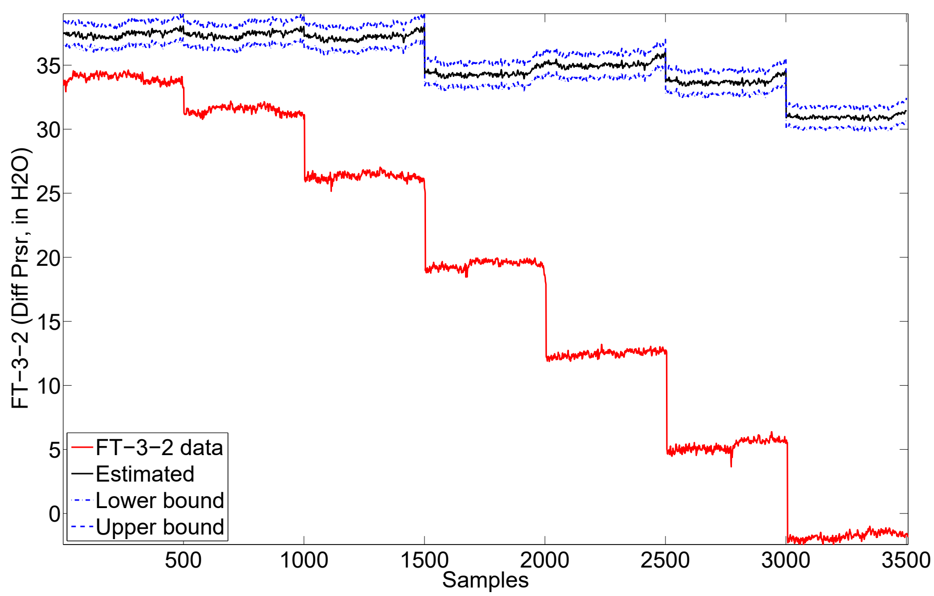

(b) input: FT-1-1

Figure 5. GP model prediction for sensor FT-3-2 measurement using a) FT-3-1 as input and b) FT-1-1 as input.

REFERENCES

1. J. Coble, P. Ramuhalli, L. Bond, J. Hines, and B. Upadhyaya, "Prognostics and health management in nuclear power plants: a review of technologies and applications," Tech. Rep. PNNL-21515, Pacific Northwest National Laboratory, Richland, WA (2012).

2. J. Hines and R. Seibert, "Technical review of on-line monitoring techniques for performance assessment. volume 1: State-of-the-art," Tech. Rep. NUREG/CR6895, U.S. Nuclear Regulatory Commission, Washington, Washington, DC 20555-0001 (2006).

3. J. Hines, D. Garvey, R. Seibert, and A. Usynin, "Technical review of on-line monitoring techniques for performance assessment. volume 2: Theoretical issues," Tech. Rep. NUREG/CR6895, U.S. Nuclear Regulatory Commission, Washington, Washington, DC 20555-0001 (2008).

4. J. Hines, J. Garvey, D. Garvey, and R. Seibert, "Technical review of on-line monitoring techniques for performance assessment. volume 3: Limiting case studies," Tech. Rep. NUREG/CR6895, U.S. Nuclear Regulatory Commission, Washington, Washington, DC 20555-0001 (2008).

5. D. K. Rollins, L. Beverlin, Y. Mei, K. Kotz, D. Andre, N. Vyas, G. Welk, and W. D. Franke, "The Development Of A Virtual Sensor In Glucose Monitoring For Non-Insulin Dependent People," *Journal of Bioinformatics and Diabetes*, **1**, 19–36 (2014).

6. C. D. Kestell, B. S. Cazzolato, and C. H. Hansen, "Active noise control in a free field with virtual sensors," *The Journal of the Acoustical Society of America*, **109**, 232–243 (2001).

7. J. W. Hines, A. V. Gribok, I. Attieh, and R. E. Uhrig, "Regularization Methods for Inferential Sensing in Nuclear Power Plants," in "Fuzzy Systems and Soft Computing in Nuclear Engineering," pp. 285–314 (2000).

8. P. Ramuhalli, G. Lin, S. L. Crawford, B. Konomi, B. G. B. J. B. Coble, B. Shumaker, and H. Hashemian, "Uncertainty quantification techniques for sensor calibration monitoring in nuclear power plants," Tech. Rep. PNNL-22847, Pacific Northwest National Laboratory, Richland, WA (2014).

9. S. Kabadayi, A. Pridgen, and C. Julien, "Virtual Sensors: Abstracting Data from Physical Sensors," in "2006 International Symposium on a World of Wireless, Mobile and Multimedia Networks," (2006), pp. 587–592.

10. J. Y. Shin, F. Kurdahi, and N. Dutt, "Cooperative On-Chip Temperature EstimationUsing Multiple Virtual Sensors," *IEEE Embedded Syst. Lett.*, **7**, 37–40 (2015).

11. T. Jin, Z. Fu, and G. Liu, "Data Mining for Soft Sensing Modeling of Power Plant Parameters," in "2009 Sixth International Conference on Fuzzy Systems and Knowledge Discovery," Institute of Electrical & Electronics Engineers (IEEE) (2009).

12. R. Tipireddy, H. Nasrellah, and C. Manohar, "A Kalman filter based strategy for linear structural system identification based on multiple static and dynamic test data," *Probabilistic Engineering Mechanics*, **24**, 60–74 (2009).

13. M. G. Na, H. Y. Yang, and D. H. Lim, "A soft-sensing model for feedwater flow rate using fuzzy support vector regression," *Nuclear Engineering and Technology*, **40**, 69–76 (2012).

14. C. E. Rasmussen and C. K. I. Williams, *Gaussian Processes for Machine Learning*, MIT Press, Cambridge, Massachusetts (2006).

15. I. Bilionis and N. Zabaras, “Multi-output local Gaussian process regression: Applications to uncertainty quantification,” *Journal of Computational Physics*, **231**, 5718–5746 (2012).

16. I. Bilionis, N. Zabaras, B. Konomi, and G. Lin, “Multi-output separable Gaussian process: Towards an efficient, fully Bayesian paradigm for uncertainty quantification,” *Journal of Computational Physics*, **241**, 212–239 (2013).

17. S. Conti and A. O’Hagan, “Bayesian emulation of complex multi-output and dynamic computer models,” *Journal of Statistical Planning and Inference*, **140**, 640–651 (2010).

18. G. Casella and E. I. George, “Explaining the Gibbs Sampler,” *The American Statistician*, **46**, 167–174 (1992).

19. N. Metropolis, A. W. Rosenbluth, M. N. Rosenbluth, A. H. Teller, and E. Teller, “Equation of State Calculations by Fast Computing Machines,” *The Journal of Chemical Physics*, **21**, 1087–1092 (1953).

20. W. K. Hastings, “Monte Carlo sampling methods using Markov chains and their applications,” *Biometrika*, **57**, 97–109 (1970).